

AN EFFECT OF THE COMBINED MICROSTRUCTURAL SIZE ON THE TENSILE
FRACTURE STRENGTH OF TWO PHASE CARBON STEEL

T. Kunio* and H. Suzuki**

1. INTRODUCTION

In many technologically important alloys, two phase microstructures having constituents of comparable sizes are often encountered [1 - 7]. In a previous paper, the authors have pointed out that the ductility of steels with combined microstructures is closely related to the connectivity¹ of the second phase by which no free deformation of the matrix is allowed [8]. This suggests that the study on the fracture strength of such a steel should be also made from the view point of microstructural aspects. However, some of the microstructural factors are still poorly understood, in particular, the effect of the size of combined microstructures of the macroscopic fracture behaviour still is unknown.

In this paper, the effect of the combined microstructural size on the tensile fracture strength will be studied, using a steel with the martensite-ferrite combined microstructures in which the connectivity on the second phase is kept constant through careful heat treatments.

2. MATERIAL AND PREPARATION OF MICROSTRUCTURES

Chemical compositions of the plain carbon steel specimens are given in Table 1. Three kinds of ferrite grain size were obtained by annealing at 1473K for one hour and then three different pre-quenching heat treatments at 1473, 1173 and 1113K for 4, 6 and 10 hours, respectively. Subsequent to the above heat treatments, the specimens were machined into the dimension as given in Figure 1. To construct a connected configuration of the second phase (martensite structure) in the specimens, the heat treatment illustrated in Figure 2 was employed. The surface microphotographs of the structures obtained by three pre-quenching heat treatments are shown in Figure 3. These microstructures are characterized from the difference in the size of the combined microstructures, such as size of ferrite grain and thickness of martensite structure. The coarsest grained material shown in Figure 3a is referred as material A, the intermediate in Figure 3b as material B and the finest in Figure 3c as material C. The data of microstructural factors obtained from a quantitative microscopic technique [9] are tabulated in Table 2. This table shows that no appreciable difference is recognized among three materials except ferrite grain size and thickness of martensite structures.

* Faculty of Engineering, Keio University, Yokohama, Japan.

** Oyama Technical College, Oyama, Japan.

1. The degree of connectivity $\bar{\psi}$ is defined by $\bar{\psi} = L_g / (L_g + L_b)$ [8], where L_g and L_b are the lengths of the boundaries of the second phase and ferrite grains including the length shared by the second phase, respectively.

3. TENSILE BEHAVIOUR OF MARTENSITE-FERRITE STRUCTURE

Static tensile tests were carried out at the room temperature to compare the tensile fracture characteristics of three materials A, B and C. Their stress-strain curves are shown in Figure 4, in which the ductility in terms of the fracture strain were appeared to be within a few percent. At the same time, it turned out from the macroscopic fracture appearance that all materials fractured in a partially brittle manner. Also, the similarities is 0.2% proof stress, strain-hardening behaviour and fracture appearance with respect to the materials A, B and C should be noted. However, the appreciable difference among the fracture strength of materials A, B and C was recognized from Figure 4.

4. EFFECT OF COMBINED MICROSTRUCTURAL SIZE ON MICROSCOPIC BEHAVIOUR OF FRACTURE

In order to study the role of the combined microstructural size in the fracture strength mentioned above, the features of microscopic fracture on the materials A and C were examined in the following. After specimens of both materials were loaded up to nearly 99% of the fracture strength, they were taken off from the test machine, and then cut, polished and nital-etched to examine the features of the internal microstructure during fracture process. At this time, the examination of three dimensional features was done by taking the photographs of microstructure at every step of successive eliminations of the surface layer by electropolishing. As a result, no appreciable difference between both materials was observed with respect to the microscopic features of the fracture. Figure 5 shows a good example of these features. Thus, it turns out that the martensite structure cracking acts as a source of cleavage microcrack in the ferrite grain and also that the propagation of cleavage microcracks is impeded by martensite structures. Consequently, it can be understood that the dimension of almost all cracks corresponds to the sum of the ferrite grain size and the thickness of the martensite structure.

5. MICROSCOPIC FEATURES OF FRACTURE SURFACES

In this section, the relation of the above microcrack to the final fracture will be examined on the fractured surfaces of materials A and C, using the scanning electron microscope (SEM). Figure 6 shows that the fracture surface was covered with dimple patterns and cleavage facets for both materials. The SEM observation (Figure 7) shows the correspondence between the fractured surface and microstructures which were revealed by the nital etching at the fractured edge [8]. It was confirmed from this photograph that the dimple pattern occurred in the martensite structure and the cleavage cracking was created in the ferrite grain. From the more detailed observation of many photographs like Figure 6 with a special attention to the river markings [10, 11], it was recognized that the final fracture is brought about by the coalescence of "the fracture process unit" which consists of a cracked second phase and cleaved ferrite grains adjacent to each other. Figure 8 is a sketch showing schematically "the fracture process unit". And it can be understood that the complete fracture was due to the coalescence of microcracks mentioned in the previous section.

6. EFFECT OF APPLIED STRESS ON MICROCRACK CREATION

For the purpose of a quantitative study on the fracture strength of the steel with the combined microstructure, the effect of applied stress on creation of the microcrack was examined in the following manner. After A and C materials were loaded and taken off from the testing machine at the certain intervals up to the fracture, the microcrack counts were made by scanning the prepared surface within the area of 1 cm² at a magnification of 400X. Figure 9 shows a ln-ln plot of the applied normal stress σ versus the number of microcrack N per unit area that is "the fracture process unit" which consists of a second phase cracking and the ferrite grain cleavage cracks. From this figure, the following relation holds for both materials

$$N = H\sigma^{1.2}$$

where H is constant. Consequently, it turns out that there exists a strong stress dependence in the creation of microcracks [12, 13, 14]. It is also noted that the number of microcracks created in the material C is more than that in A. This fact may imply that the shorter the sum of ferrite grain size and martensite structural thickness adjacent to each other becomes, the harder their coalescences of microcracks are. Therefore, it is interpreted that the fracture strength of present two phase carbon steel is affected remarkably by the coalescence of microcracks represented by "the fracture process unit".

7. CONCLUSIONS

A study was made on the fracture strength of the materials with martensite (second-phase)-ferrite (matrix phase) microstructure which have identical structure properties except the combined microstructural size. The results obtained are summarized as follows.

- (1) The fracture strength of the present materials are strongly dependent on the size of the combined microstructures, whereas the plastic properties are independent of it.
- (2) The final fracture is brought about by the coalescence of "the fracture process unit" which consists of the cracked second phase and the adjacent cleavage ferrite grains.
- (3) The effect of the combined microstructural size on the fracture strength can be explained through the size of "the fracture process unit" which is dependent on the combined microstructural size.

ACKNOWLEDGEMENTS

The authors are indebted to Dr. M. Shimizu and Dr. K. Yamada of Keio University for valuable discussions. Gratitude is also expressed to Mr. A. Nishimura and the Staff of the Materials Science Laboratory, Keio University for their assistance with experimental works.

REFERENCES

1. TAMURA, I., Bull. Japan Inst. Met., 15, 1976, 647.
2. SUZUKI, H. and KUNIO, T., Bull. Japan Inst. Met., 15, 1976, 665.
3. HAYDEN, H. W. and FLOREEN, S. F., Trans. ASM, 61, 1968, 474.
4. HAYDEN, H. W. and FLOREEN, S. F., Met. Trans., 1, 1970, 1955.
5. CHENG, I. L. and THOMAS, G., Met. Trans., 3, 1972, 503.
6. GURLAND, J. and PARIKH, N. M., "Fracture", edited by H. Liebowitz, Academic Press, New York, 1972, 841.
7. TOMODA, Y., KUROKI, G. and TAMURA, I., J. Iron Steel Inst., Japan, 61, 1975, 107.
8. KUNIO, T., SHIMIZU, M., YAMADA, K. and SUZUKI, H., Eng. Frac. Mech., 7, 1975, 411.
9. "Quantitative Microscopic", edited by R. T. Dehoff and F. N. Rhines, McGraw-Hill, New York, 1968.
10. BEACHEM, C. D., "Fracture", edited by H. Liebowitz, Academic Press, New York, 1, 1972, 243.
11. TERASAKI, F. and KANEKO, T., J. Iron and Steel Inst., Japan, 60, 1974, 1599.
12. HAHN, G. T., HOAGLANG, R. G. and ROSENFELD, A. R., Met. Trans., 2, 1971, 535.
13. LINDLEY, T. G., OATES, G. and RICHARDS, C. E., Acta Met., 18, 1970, 1127.
14. KAECELE, L. E. and TETELMAN, A. S., Acta Met., 17, 1969, 463.

Table 1 Chemical Composition

C	Si	Mn	S	P
0.25	0.24	0.43	0.035	0.030

Table 2 Microstructural Factors

	Martensite Structure				Ferrite Grain	
	Volume Fraction, %	Hardness H_V	Connectivity %	Thickness μm	Hardness H_V	Size μm
A	44	665	95	36	197	62
B	45	698	97	26	197	43
C	42	640	94	13	200	24

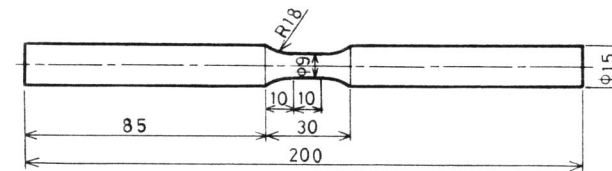


Figure 1 Dimensions of Specimen

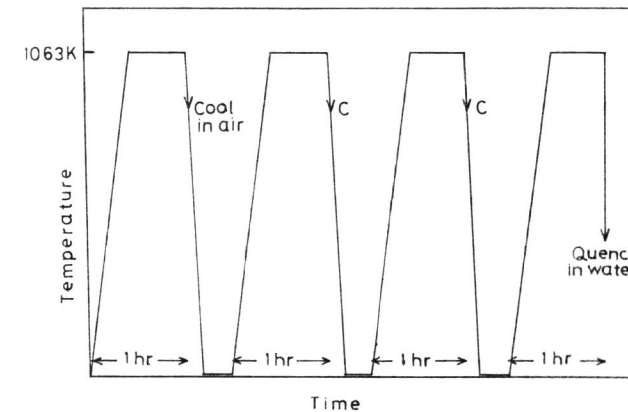


Figure 2 Process of the Heat Treatment

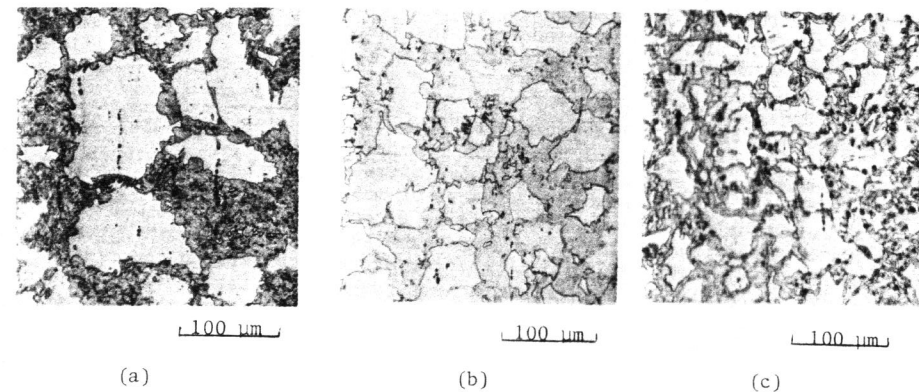


Figure 3 Microstructures for (a) Material A; (b) Material B; (c) Material C

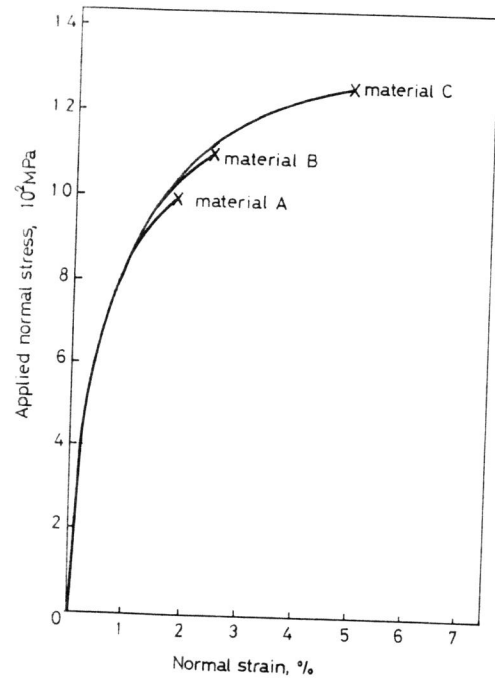
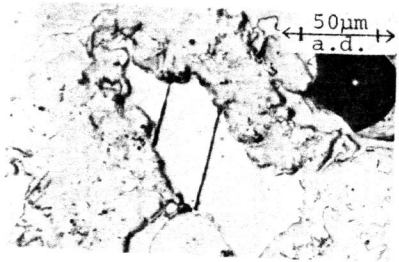
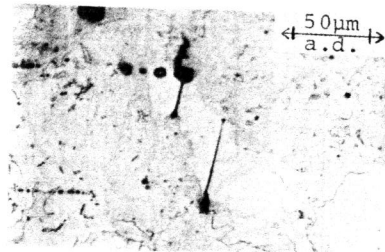


Figure 4 Stress-Strain Curves

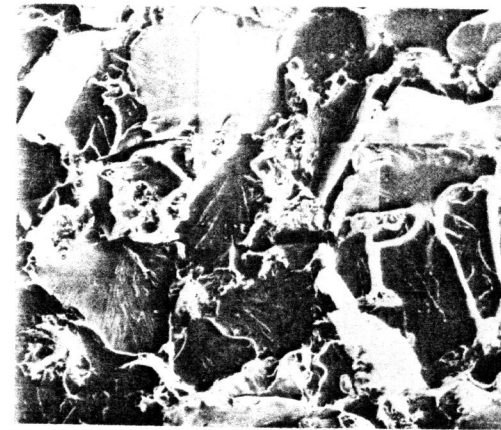


(a)

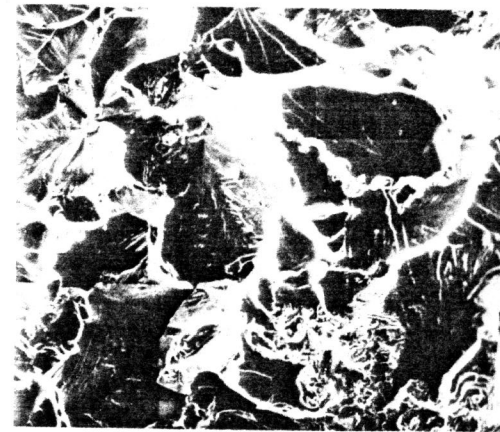


(b)

Figure 5 Cleavage Cracks Initiated by Cracked Second Phase Appeared on Figure 5b Surface Which is 21 μm Beneath Figure 5a Surface



(a)



(b)

Figure 6 Scanning Electron Fractographs for (a) Material A; (b) Material C

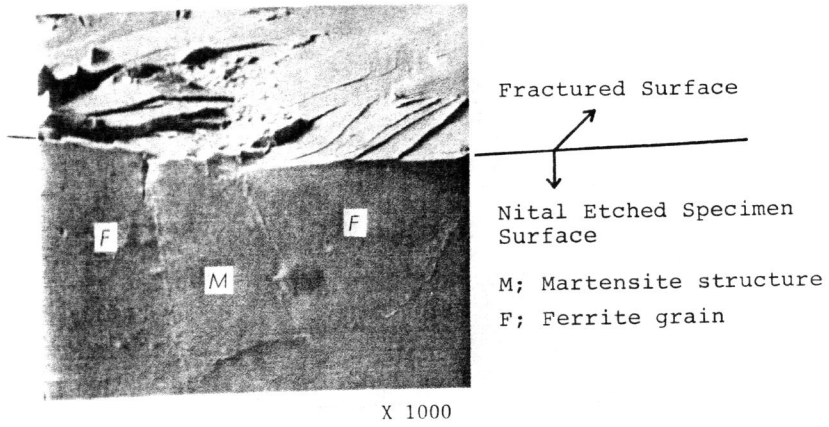
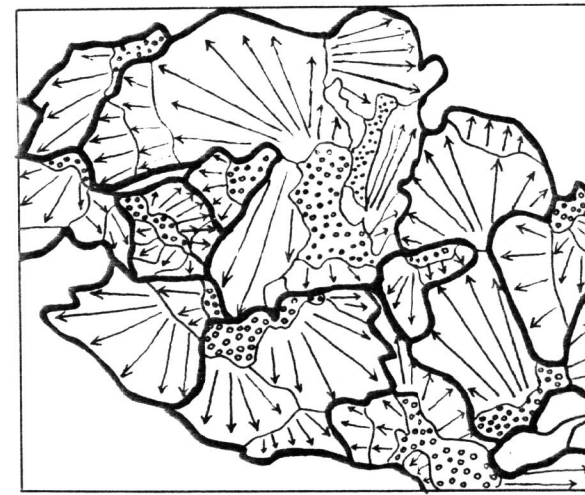


Figure 7 Scanning Electron Fractograph Showing the Correspondence Between the Fractured Surface and the Microstructures






(a)



(b)

Figure 8 Schematic Illustration of the Fracture Surface Covered with the Dimple Pattern and Cleavage Facets with River Markings in (a) Material A; (b) Material C. Arrows Indicate the Direction of the Microcrack Propagation

 the fracture process unit.
  the dimple pattern.
  the cleavage facets.

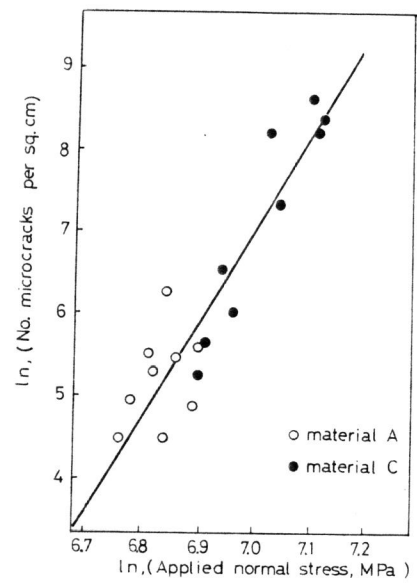


Figure 9 Number of Microcracks per Sq. Cm as a Function of Applied Normal Stress (MPa)